

## MULTI-FEATURE BASED DETECTION OF LANDMINES USING GROUND PENETRATING RADAR

Kyungmi Park, Suncheol Park, Kangwook Kim, and Kwang Hee Ko\*

School of Mechatronics, Gwangju Institute of Science and Technology, Gwangju, Republic of Korea

**Abstract**—In this paper, we present a method for detecting anti-tank or anti-personnel landmines buried in the ground. A set of data generated by a ground penetrating radar is processed to remove the surface reflection and clutter, yielding signals for possible landmines. In order to detect landmines in the signals, features are computed and compared against a database, which contains those of various landmines. Three features are proposed to use; principal components from principal component analysis, Fourier coefficients and singular values from singular value decomposition method, each of which is chosen to represent each landmine uniquely. Detection is performed using Mahalanobis distance-based method. Examples show that the proposed method can effectively detect landmines in various burial condition.

### 1. INTRODUCTION

Search and removal of landmines is a serious problem faced by many countries. Annually more than 20,000 people all over the world are getting injured or losing their lives because of landmine accidents. However, the victims are not only restricted to soldiers. Recent heavy rain with floods and landslides may move landmines to civilian areas, threatening civilians' safety [1, 2]. Therefore, safe and efficient removal of landmines is critical.

Removal of landmines requires detection, which can be done in various ways [1, 3], and a method to detect without digging the ground is preferable for a safety reason. Metal detectors can be used for this purpose [3–5]. However, many landmines are made of plastic

---

*Received 4 October 2012, Accepted 3 December 2012, Scheduled 6 December 2012*

\* Corresponding author: Kwang Hee Ko (khko@gist.ac.kr).

or may have low metal content, which limits the effectiveness of the method in practice. To handle such landmines a ground based X-band scatterometer [6] can be considered. Or radar is another option.

Radar has been successfully employed for detection of various entities such as breast cancers [7–9], hidden objects or humans [10–19], moving targets [20–22] and their speed [23,24] and speech acquisition [25]. Among various types of radars developed so far, ground penetrating radars (GPRs) have attracted many researchers attention. GPRs have been used for various applications such as [26,27] and [28], to name a few.

In particular, they are frequently selected for landmine detection [2,29–33]. In addition, an attempt to use a metal detector and a GPR together in the landmine detection has been made [34].

In this paper, detection of a landmine using GPR only is a primary focus. Landmine detection consists of three steps: reduction of clutter, feature extraction and decision. When a GPR signal is obtained, clutter, such as noise in the signal and reflections from the ground and other objects, needs to be removed to obtain part of the signal for feature extraction step [30,35–37].

Features corresponding to a landmine are extracted from the signal with reduced clutter. Various types of features are proposed in order to obtain features unique to a landmine. Features can be extracted in either time or frequency domain [29,32,33,38]. Once features of a landmine are available, they are compared with those in a database containing landmine features and the associated information of various landmines and burial conditions. It is unlikely to have the perfect match against the features in the database due to uncertainty involved in the GPR signal. Therefore, a systematic decision algorithm needs to be employed. For a robust decision, methods such as hidden Markov models [32,39], Mahalanobis distance [33] and Support Vector Machine [40] are studied. Wilson et al. [41] review four algorithms for landmine detection and discrimination using GPR: hidden Markov model (HMM) algorithm, geometric feature FOWA ROCA algorithm, spectral confidence feature algorithm and edge histogram discrimination algorithm. Their evaluation shows that among the four methods HMM and edge histogram discrimination algorithms provide the superior overall performance. They also note that fusion of more than two different algorithms could enhance the performance. In relation to this comment, use of multiple features for landmine detection is addressed in [33,42].

In this paper, a novel landmine detection algorithm is proposed. Using devices currently employed in practice, any object in the ground could be detected. The false alarm rate using the existing

methods, however, still remains high, which is as problematic as a low detection rate in the landmine removal. Therefore, the goal of this work is to lower the false alarm rate by identifying an object in the signal to be a landmine or not using the proposed method. A new approach for isolating landmine signals is presented for robust feature extraction. Moreover, use of multiple features including singular values from singular value decomposition, Fourier coefficients and principal components from principal component analysis are proposed to enhance differentiability of landmines in order to improve the detection rate. The overall landmine detection process is given as follows. The GPR data is processed to eliminate clutter in the signal, yielding signals containing a possible landmine. From the signal, features based on the three methods are extracted, which are then compared with those in the database for detection and identification. For decision, Mahalanobis distance based method is employed for features in multidimensional space.

The paper is structured as follows: In Section 2, preprocessing steps for eliminating the ground effects and clutter are presented. In Section 3, the three feature extraction methods are proposed along with the decision scheme using Mahalanobis distance based approach in Section 4. The proposed methods are tested with examples in Section 5. Section 6 concludes this paper with suggestions and future work.

## 2. PRE-PROCESSING

### 2.1. GPR Data

A GPR scans the ground and generates data, which contain influences from the target object as well as the ground of various conditions and other obstacles. One example of GPR data is given in Fig. 1. The  $x$ -axis is the width (mm) of the scanning area, the  $y$ -axis is the depth (mm) of the ground and the  $z$ -axis is the signal strength in voltage.

The GPR system used in this work is Minehound VMR2 from COBHAM, which is configured as shown in Fig. 2. The antenna is designed to move horizontally covering the area while maintaining a certain distance from the ground surface.

### 2.2. Extraction of Landmine Signals

The GPR data ( $\mathbf{D}$ ) is assumed to consist of three different components: reflection from the ground ( $\mathbf{G}$ ), reflection from a buried landmine ( $\mathbf{L}$ ) and clutter ( $\mathbf{N}$ ), which are linearly combined [43]. Therefore, in order to obtain landmine signals, the signals  $\mathbf{G}$  and  $\mathbf{N}$  should be eliminated.

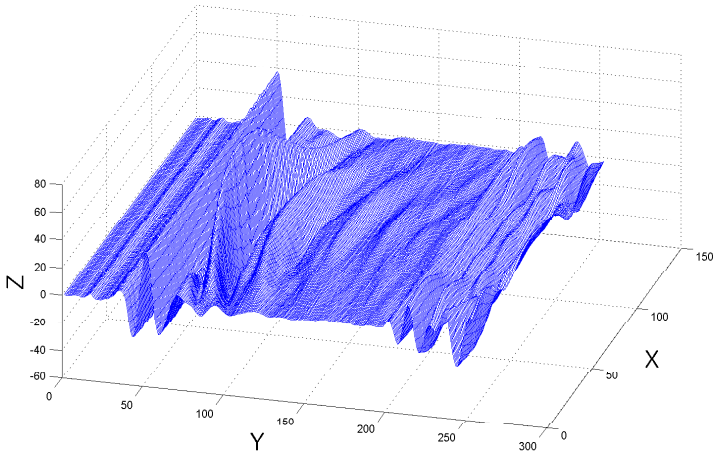


**Figure 1.** An example of GPR data.

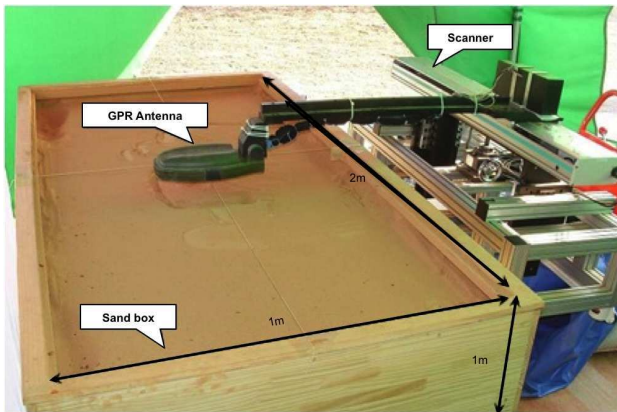


**Figure 2.** The GPR system used in the experiment.

Theoretically, the ground effect is removed by subtracting  $\mathbf{G}$  from  $\mathbf{D}$ . Two subtraction steps are proposed for extracting  $\mathbf{L}$ . The first step is to subtract average signals for  $\mathbf{G}$  and  $\mathbf{N}$  from  $\mathbf{D}$ . The average of  $\mathbf{G}$  can be obtained by averaging the signals of various grounds with no landmine. The averaged signal is called the reference data. Consider  $n$  ground conditions with no landmine contained. Then there exist  $n$  ground signals  $\mathbf{G}_i + \mathbf{N}_i$  ( $i = 1, \dots, n$ ). Suppose that  $E[\cdot]$  is the notation of average computation. The average of them,  $\mathbf{S}^*$ , is obtained by

$$\mathbf{S}^* = E[\mathbf{G}_i + \mathbf{N}_i] = E[\mathbf{G}_i] + E[\mathbf{N}_i] = \mathbf{G}^* + \mathbf{N}^*. \quad (1)$$

Therefore,

$$\begin{aligned}
 \mathbf{D} - \mathbf{S}^* &= \mathbf{G} + \mathbf{L} + \mathbf{N} - (\mathbf{G}^* + \mathbf{N}^*), \\
 &= \mathbf{L} + \Delta\mathbf{G} + \Delta\mathbf{N}, \\
 &= \mathbf{L} + \mathbf{R}.
 \end{aligned}
 \tag{2}$$

In this computation,  $\mathbf{R}$  remains to be nonzero since  $\Delta\mathbf{G}$  and  $\Delta\mathbf{N}$  hardly become zero in general. This process is illustrated in Fig. 3, where Figs. 3(a), (b) and (c) are the input signal, the signal without a landmine and the signal after subtraction. The residue signal  $\mathbf{R}$  in Fig. 3(c) needs to be minimized in order to obtain  $\mathbf{L}$  for the downstream processes, which is performed in the second subtraction step. In this step, the result of the first subtraction step, (i.e., Fig. 3(c)), is used as input. The data at each  $x$  are squared, and the sum of the squared values is computed. Among the summation values, the signal corresponding to the smallest one is selected, which is then subtracted

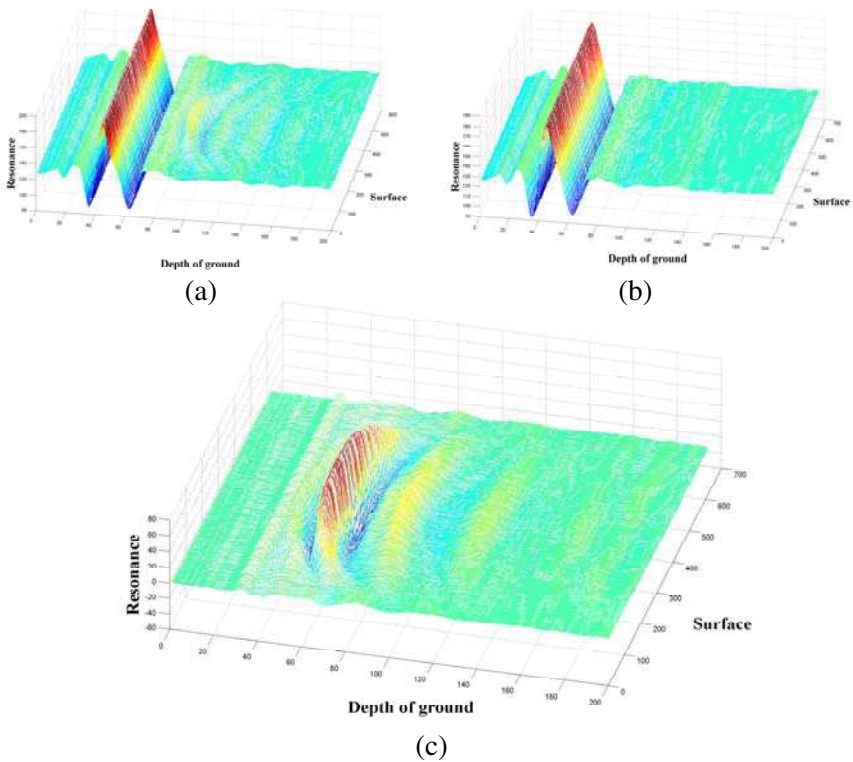


**Figure 3.** Illustration of the subtraction process. (a) The input signal, (b) the signal without an object in the ground and (c) the result of the subtraction steps.

from the signals at all  $x$ . These two subtraction steps yield a signal  $\mathbf{L}_u = \mathbf{L} + \mathbf{R}_u$ , where  $\mathbf{R}_u$  is a residue survived the two subtraction steps. Once  $\mathbf{L}_u$  is available, Kalman filter method is employed in the  $y$  direction. The residue  $\mathbf{R}_u$  is treated as clutter, which can be eliminated by the filter with minimally changing the landmine signal. The signal  $\mathbf{L}_{ui}$  at each  $x_i$  is regarded as a function of time. Namely, the  $y$  axis is the time axis. Under this assumption, Kalman filter can be employed to reduce  $\mathbf{R}_{ui}$  to yield  $\mathbf{L}$ .

### 2.3. Kalman Filter

Kalman filter is one of the most frequently used methods for signal processing in various applications and in many cases, it is used for such as removing noise or clutter [44, 45] and tracking [46–48].

Kalman filter is effective in removing noise or clutter in the GPR signal, which can be modeled as Gaussian noise. It is considered as

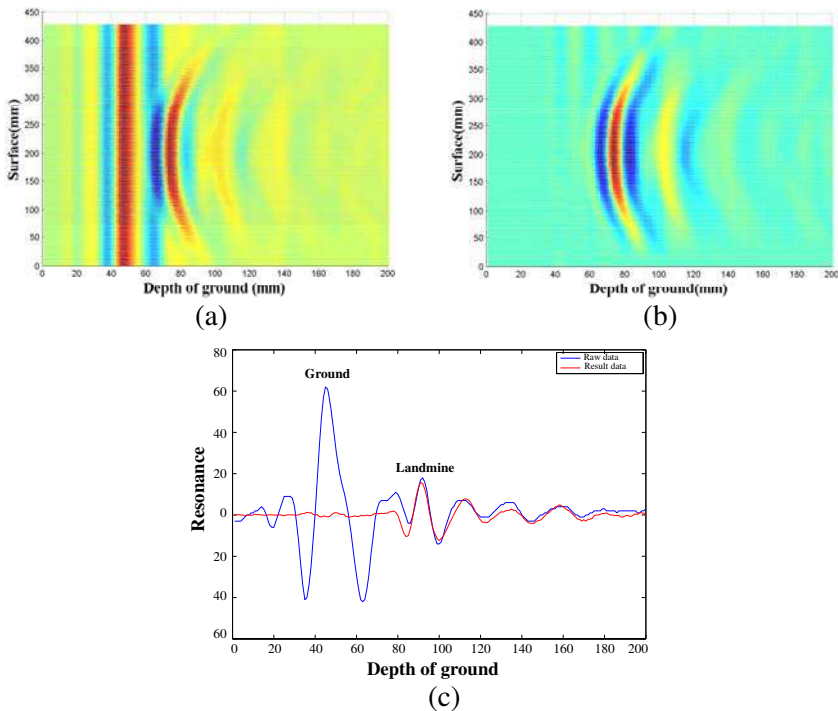


**Figure 4.** Illustration of the second clutter reduction, (a) is the processed signal  $\mathbf{L} + \mathbf{R}$ , (b) is the signal  $\mathbf{L}$  after the clutter is reduced, (c) is the comparison of signals before and after the ground and clutter reduction process.

a predictor-corrector scheme, which predicts states using data in the previous time, and corrects the prediction based on measurement at the current time. The process and measurement noise models are assumed to have normal probability distribution. The residue in the signal can be effectively reduced using this approach. Fig. 4 shows the result of the ground and clutter reduction. As shown in the figure, the ground component is efficiently eliminated without disturbing the landmine part compared with the input raw data.

The extracted signal  $\mathbf{L}$  is then normalized to linearly scale the signal to the range of  $-100$  to  $100$ . Through this normalization, various factors affecting signal strength such as the ground materials, moisture levels and the height of the GPR, can be eliminated to make the feature extraction more reliable.

### 3. FEATURE EXTRACTION

The extracted signal  $\mathbf{L}$  is processed for feature extraction. In this section, three different methods are presented, producing three features for one landmine: Principal Component Analysis, Singular Value Decomposition and Fourier transform. The first two methods use data in the spatial domain, whereas the last one is based on data in the frequency domain. Therefore, combining the three methods would provide a way to extract features with enhanced differentiability for detection compared to using a less number of methods such as [42], where PCA and FE are considered. Using each feature for one axis, 3D space, called the feature space, is defined, in which a landmine is mapped to one point.

#### 3.1. Principal Component Analysis (PCA)

PCA extracts patterns of a scattered data set in  $K$ -dimension. The patterns are captured in the eigenvalues and eigenvectors of a  $K \times K$  covariance matrix. A pair of an eigenvector and an eigenvalue shows how strong a pattern the data point contains in the eigenvector direction. Therefore, it can be used as a unique feature of each landmine. PCA has been used for a wide spectrum of applications such as [49–53]. In this work, it is used for landmine identification. In order to apply this method, the extracted signal is projected onto the  $x$ - $z$  plane as shown in Fig. 5. Then, the eigenvector along with its eigenvalue close to the  $z$  direction is chosen as a feature since this eigenvalue shows better differentiability than the eigenvalue in the other direction.

### 3.2. Singular Values Decomposition (SVD)

As a second feature, singular values obtained from the singular value decomposition method are considered. They are used for analyzing data such as images by representing them based on characteristic values. The signal  $\mathbf{L}$  is represented by a matrix of intensity of a signal at each position. In order to improve the differentiability of singular values, a method, called the window scanning, is proposed. Consider a signal  $\mathbf{L}$  as shown in Fig. 6. A window restricting the domain of interest, which is illustrated as a rectangle in the left image of Fig. 6(a), is applied to  $\mathbf{L}$  to obtain data focusing on a possible landmine as shown in the right image of Fig. 6. This process eliminates unnecessary part

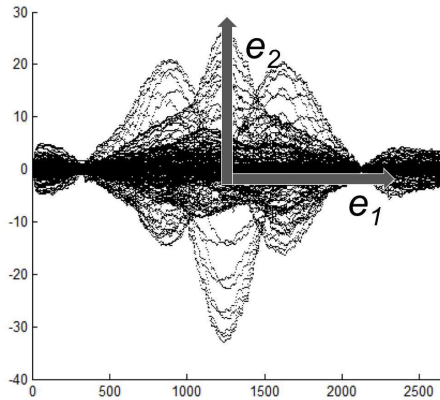


**Figure 5.** The signal projected onto  $x$ - $z$  plane.  $e_1$  and  $e_2$  are the two eigenvectors.

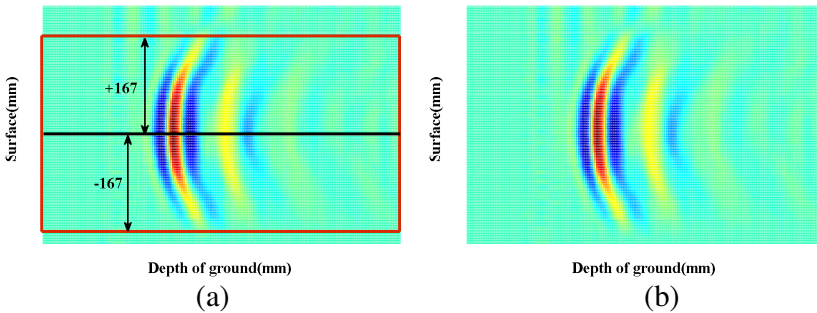


**Figure 6.** Illustration of the window scanning method. The height of the window is determined to be 334 in this example.

outside the window, leaving data concentrating on a possible landmine. The size of the window is automatically determined to be large enough to contain the signal of a landmine having the largest reflection. The window is placed in such a way that the centerline of the window matches the position of the maximum signal strength.

The data inside the window is provided for SVD. Once singular values are computed, the largest one is chosen as a feature of the landmine in the data because the largest singular value is robust with respect to small perturbation to the input signal.

### 3.3. Discrete Fourier Transform (DFT)

As a third feature, a Fourier coefficient at a certain frequency is considered. Unlike the previous two methods, which are based on data in the spatial domain, this approach represents the data in the frequency domain, which would capture different aspects of the input signal. Since the input signal is given in discrete form, a discrete version of Fourier transform is used. Fourier transform is a fundamental mathematical tool for signal processing and matching and finds an enormous amount of applications such as radar data processing [54], polynomial construction [55], design of devices [56], target recognition [57] and landmine detection [58], to name a few.

In order to apply DFT, a row of signal corresponding to the largest

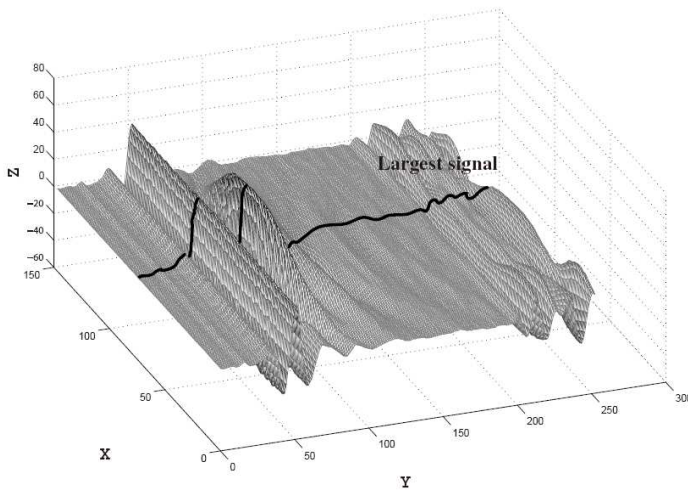


**Figure 7.** An example of a signal with the largest strength indicated as a thick curve in the figure. This signal is provided as input to DFT for feature extraction.

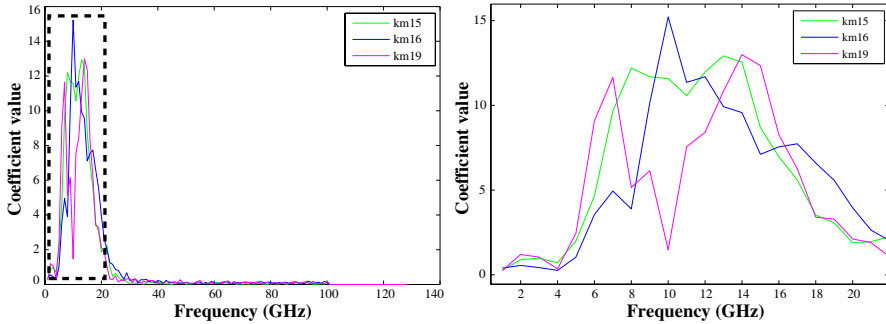


**Figure 8.** Results of DFT for three different landmine signals. The rectangular area in the left image is depicted in the right.

strength as illustrated in Fig. 7 is selected as input to DFT. Fig. 8 shows an example of DFT for three different landmines. The frequency range of the radar used in this work is from 60 MHz to 8.06 GHz. Therefore, the frequency components in that range are dominant in the frequency domain.

In order to use the Fourier coefficients as features, frequencies at which the corresponding coefficients do not overlap are chosen as features. In this work, the frequencies of 0.39 GHz, 0.47 GHz and 0.55 GHz are considered depending on the ground condition after investigating the DFT results for all the landmines and the ground conditions.

#### 4. DECISION ALGORITHM

Once features are extracted from input signals, they are compared with those in the database in order to determine whether input features correspond to a certain landmine and if so what type the landmine is. For this purpose, a database is constructed to contain features and information for various landmines, burial depths and burial conditions. Then, by finding the features similar to input, the most probable landmine is retrieved. In general, it is almost impossible to have the perfect match of features due to clutter and disturbances in the signal. Therefore, a systematic method to search the best one should be considered in order to improve the detection performance.

In this work, Mahalanobis distance concept is employed for decision. Features of a landmine correspond to one point in the feature space, whose  $x$ ,  $y$  and  $z$  axes are the second eigenvalues, the DFT coefficients and the singular values given in terms of energy,

respectively. The database can be visualized as clustered points in the feature space as is shown in Fig. 9.

An input signal will be mapped to a point in the feature space. The closest group to the input point in the statistical sense would be chosen as the target landmine. Mahalanobis distance method finds the closest cluster to the input point. It considers the relation between the standard deviation and the input data, which is used to determine the similarity of the input cluster to the existing set of clusters. Since the data patterns in each cluster are considered, Mahalanobis distance concept is different from Euclidean distance method.

A Mahalanobis distance,  $M_{\max}$ , is determined from a series of experiments, which indicates the maximum Mahalanobis distance giving the correct landmine identification. This means that an object with Mahalanobis distance less than or equal to  $M_{\max}$  is determined to be a landmine. Therefore, a database needs to be constructed to contain information on as many landmines as possible in order to maintain the high detection rate.

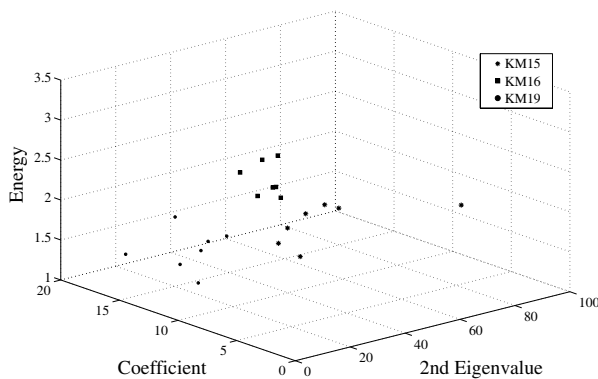


**Figure 9.** An example of feature plots in 3D space. Three landmines are considered for the dry sand ground.



**Figure 10.** The landmines used in the experiments. From the left, each landmine is KM15, KM16 and KM19, respectively.

## 5. EXPERIMENTS

In this work, three landmines: KM15, KM16 and KM19 as shown in Fig. 10 are used to test the proposed detection method. The specification of each landmine is summarized in Table 1.

The setup for this experiment is given in Fig. 2. Three ground materials, sand, gravel and soil, are used with three different moisture levels, wet, moderate and dry. Landmines are buried in the ground at 0 cm through 30 cm with 5 cm interval. The radar is positioned at the height of 6 cm from the ground surface. The robot arm moves horizontally generating  $153 \times 253$  data points.

Figures 9, 11 and 12 show features of the landmines buried in the sand with dry, moderate and wet moisture levels. It is observed that each landmine of the same type buried at different depths (from 0 cm to 30 cm) forms clusters in the feature space for each moisture level. These figures are shown separately for an illustration purpose. In the database used by the proposed method, one feature space is constructed containing features for all the landmines buried in all the ground conditions. The feature space is then used for identification and classification.

**Table 1.** Specification of the landmines.

Spec.	KM15	KM16	KM19
Size (mm)	$333 \times 150$	$102 \times 127$	$332 \times 94$
Material	Metal	Metal	Plastic

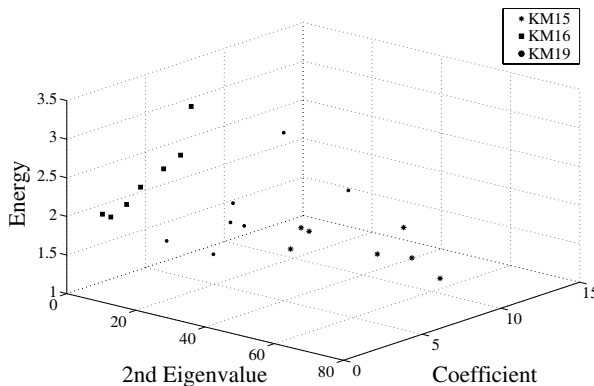


**Figure 11.** A feature plot for the sand with moderate moisture level.

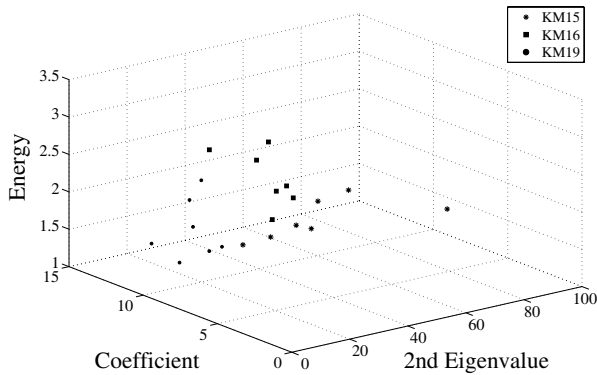


**Figure 12.** A feature plot for the wet sand.

**Table 2.** Comparison of detection between Euclidean Distance and Mahalanobis Distance methods. The unit is %.

Ground	Method	1%	5%	10%	15%	20%	25%	30%
Dry sand	EUD	85.71	94.76	85.71	85.71	71.43	47.62	42.86
	MAD	95.24	95.24	100.00	95.24	95.24	85.71	52.38
Dry Soil	EUD	100.00	100.00	100.00	89.52	47.62	47.62	38.10
	MAD	95.24	95.24	94.76	95.24	94.76	85.71	61.90
Dry Gravel	EUD	89.52	85.71	71.43	47.62	23.81	33.33	33.33
	MAD	95.24	95.24	95.24	85.71	85.71	66.67	66.67
Moderate Sand	EUD	66.67	89.52	95.24	89.52	57.14	47.62	38.10
	MAD	94.76	85.71	89.52	71.43	66.67	66.67	61.90
Moderate Soil	EUD	33.33	38.10	42.86	38.10	71.43	42.86	33.33
	MAD	66.67	66.67	61.90	66.67	61.90	61.90	42.86
Moderate Gravel	EUD	89.52	89.52	76.19	71.43	71.43	71.43	38.10
	MAD	89.52	76.19	61.90	61.90	57.14	57.14	61.90
Damp Sand	EUD	89.52	94.76	95.24	85.71	61.90	52.38	47.62
	MAD	94.76	85.71	89.52	76.19	71.43	76.19	71.43
Damp Soil	EUD	33.33	42.86	47.62	33.33	38.10	38.10	38.10
	MAD	71.43	94.76	85.71	66.67	52.38	52.38	47.62
Damp Gravel	EUD	66.67	66.67	76.19	89.52	71.43	47.62	42.86
	MAD	94.76	94.76	89.52	89.52	61.90	61.90	71.43

In order to simulate the field signals, random Gaussian noise of 1% to 30% is added to the input. Then features are computed using the proposed method. These cases are tested with the database in order to evaluate the performance of the proposed method. For comparison, Euclidean distance decision method is considered. This method finds the closest group to the input in terms of Euclidean distance in the feature space and retrieves corresponding landmine information.

Table 2 summarizes the results of detection for various cases. Here, EUD and MAD indicate Euclidean and Mahalanobis distance methods,

respectively. It is noticed that as the noise level grows, the detection rate decreases. However, Mahalanobis distance detection method works much superior to Euclidean distance method. In particular at a high noise level, the rate is mostly over 50%, which demonstrates that Mahalanobis distance method is robust with respect to noise.

Compared with the method in [42, 58], which uses two features for identification, it is found that the proposed method outperforms the previous one in most cases. Especially, the performance gap grows as the level of noise is increased. For example, the success identification rate of the proposed method with 30% noise is 61.90% as opposed to 27.78% of the previous one for the sand ground condition. Such improvements of the rate of success have been achieved by using the enhanced clutter reduction methods and using more features in the decision step.

## 6. CONCLUSION

In this paper, a novel method for landmine detection is presented. The procedure consists of data preprocessing, feature extraction and detection. Data are obtained by using a GPR. They are then processed in order to reduce unnecessary signals in order to isolate signals for landmines. Three features based on SVD, DFT and PCA, are extracted to each signal for landmine detection, which is performed by using Mahalanobis distance method. The proposed procedure is tested with three different landmines and various ground conditions.

In this work, three features are proposed for landmine signatures. Two of them, SVD and PCA, are based on data in the time domain, whereas DFT captures features in the frequency domain. Using multiple features is advantageous in the landmine detection since features extracted by using different methods may reflect different aspects of the signal, which can be more tolerant against certain disturbances than the others. This property can improve the differentiability between landmines in various burial conditions and enhance the robustness of the detection process.

For decision, Mahalanobis distance method is used in the work. The method is selected over an HMM based algorithm since it is simple to implement and applied to the proposed framework in a straightforward manner, and the features extracted in the process may not be rigorously treated independent in the probabilistic sense, which is not a suitable condition for the HMM based method. Even though such aspects are considered, however, an HMM based algorithm is worth to try in the proposed framework.

The validation has been performed under the experimental conditions. With artificial disturbances added to the signal in order to

simulate the real environment, the proposed procedure could identify correct landmines in most cases. However, it needs to be tested under the real field conditions for thorough evaluation. Some components used in the method need to be adjusted and verified in order for the proposed method to be used for live ammunition. Moreover, if the ground has a rough surface such as in the real field, or if part of a landmine is embedded in a rough surface, a reflection pattern from the ground, which is significantly different from that considered in this work, would be obtained. For this case, methods such as [59] and [60] needs to be taken into account in the proposed method. It is expected that if the proposed method is evaluated and refined through extensive tests with various landmines and ground conditions, the false alarm rate could be further reduced.

The thorough validation as well as application of an HMM based algorithm, are recommended for future work.

## ACKNOWLEDGMENT

This work was supported by the Unmanned Technology Research Center, Defense Acquisition Program Administration, and Agency for Defense and Development, Daejeon, Korea and by the Basic Research Project through a grant provided by GIST, 2012.

## REFERENCES

1. Robledo, L., M. Carrasco, and D. Mery, "A survey of land mine detection technology," *Int. J. Remote Sens.*, Vol. 30, No. 9, 2399–2410, 2009.
2. Ho, K. C. and P. D. Gader, "A linear prediction land mine detection algorithm for hand held ground penetrating radar," *IEEE Trans. Geosci. Remote Sens.*, Vol. 40, No. 6, 1374–1384, 2002.
3. Tran, M. D. J., C. Abeynayake, L. C. Jain, and C. P. Lim, "An automated decision system for landmine detection and classification using metal detector signals," *Stud. Comput. Intell.*, Vol. 304, 175–200, 2010.
4. Collins, L., P. Gao, D. Schofield, J. Moulton, L. Makowsky, D. Reidy, and R. A. Weaver, "Statistical approach to landmine detection using broadband electromagnetic induction data," *IEEE Trans. Geosci. Remote Sens.*, Vol. 40, No. 4, 950–962, 2002.
5. Won, I. J., D. A. Keiswetter, and T. H. Bell, "Electromagnetic induction spectroscopy for clearing landmines," *IEEE Trans. Geosci. Remote Sens.*, Vol. 39, No. 4, 703–709, 2001.

6. Tiwari, K. C., D. Singh, and M. K. Arora, "Development of a model for detection and estimation of depth of shallow buried non-metallic landmine at microwave x-band frequency," *Progress In Electromagnetics Research*, Vol. 79, 225–250, 2008.
7. Alshehri, S. A., S. Khatun, A. B. Jantan, R. S. A. Raja Abdullah, R. Mahmood, and Z. Awang, "Experimental breast tumor detection using NN-based UWB imaging," *Progress In Electromagnetics Research*, Vol. 111, 447–465, 2011.
8. Alshehri, S. A., S. Khatun, A. B. Jantan, R. S. A. Raja Abdullah, R. Mahmood, and Z. Awang, "3D experimental detection and discrimination of malignant and benign breast tumor using NN-based UWB imaging system" *Progress In Electromagnetics Research*, Vol. 116, 221–237, 2011.
9. O'Halloran, M., B. McGinley, R. C. Conceicao, F. Morgan, E. Jones, and M. Glavin, "Spiking Neural Networks for breast cancer classification in a dielectrically heterogeneous breast," *Progress In Electromagnetics Research*, Vol. 113, 413–428, 2011.
10. Chang, Y.-L., C.-Y. Chiang, and K.-S. Chen, "SAR image simulation with application to target recognition," *Progress In Electromagnetics Research*, Vol. 119, 35–57, 2011.
11. Jia, Y., L. Kong, and X. Yang, "A novel approach to target localization through unknown walls for through-the-wall radar imaging," *Progress In Electromagnetics Research*, Vol. 119, 107–132, 2011.
12. Burgos-Garcia, M., F. Perez-Martines, and J. Gismero Menoyo, "Radar signature of a helicopter illuminated by a long LFM signal," *IEEE Trans. Aerosp. Electron. Syst.*, Vol. 45, 1104–1110, 2009.
13. Davy, M., T. Lepetit, J. de Rosny, C. Prada, and M. Fink, "Detection and imaging of human beings behind a wall using the DORT method," *Progress In Electromagnetics Research*, Vol. 110, 353–369, 2010.
14. Ray, P. and P. K. Varshney, "Radar target detection framework based on false discovery rate," *IEEE Trans. Aerosp. Electron. Syst.*, Vol. 47, 1277–1292, 2011.
15. Zhang, H., S. Y. Tan, and H. S. Tan, "Experimental study on a flanged parallel-plate dielectric waveguide probe for detection of buried inclusions," *Progress In Electromagnetics Research*, Vol. 111, 91–104, 2011.
16. Debes, C., A. M. Zoubir, and M. G. Amin, "Enhanced detection using target polarization signatures in through-the-wall radar imaging," *IEEE Trans. Geosci. Remote Sensing*, Vol. 50, 1968–

- 1979, 2012.
17. Mohammadpoor, M., R. S. A. Raja Abdullah, A. Ismail, and A. F. Abas, "A circular synthetic aperture radar for on-the-ground object detection," *Progress In Electromagnetics Research*, Vol. 122, 269–292, 2012.
  18. Hatam, M., A. Sheikhi, and M. A. Masnadi-Shirazi, "Target detection in Pulse-train MIMO radars applying ICA algorithms," *Progress In Electromagnetics Research*, Vol. 122, 413–435, 2012.
  19. Wang, Y., Q. Song, T. Jin, Y. Shi, and X.-T. Huang, "Sparse time-frequency representation based feature extraction method for landmine discrimination," *Progress In Electromagnetics Research*, Vol. 133, 459–475, 2013.
  20. Tian, B., D.-Y. Zhu, and Z.-D. Zhu, "A novel moving target detection approach for dual-channel SAR system," *Progress In Electromagnetics Research*, Vol. 115, 191–206, 2011.
  21. Guan, J., X.-L. Chen, Y. Huang, and Y. He, "Adaptive fractional Fourier transform-based detection algorithm for moving target in heavy sea clutter," *IET Radar, Sonar and Navig.*, Vol. 6, 389–401, 2012.
  22. Budillon, A., A. Evangelista, and G. Schirinzi, "GLRT detection of moving targets via multibaseline along-track interferometric SAR system," *IEEE Geosci. Remote Sens. Lett.*, Vol. 9, 348–352, 2012.
  23. Mao, X., D.-Y. Zhu, L. Ding, and Z.-D. Zhu, "Comparative study of RMA and PFA on their responses to moving target," *Progress In Electromagnetics Research*, Vol. 110, 103–124, 2010.
  24. Sjogren, T. K., V. T. Vu, M. I. Pettersson, A. Gustavsson, and L. M. H. Ulander, "Moving target relative speed estimation and refocusing in synthetic aperture radar images," *IEEE Trans. Aerosp. Electron. Syst.*, Vol. 48, 2426–2436, 2012.
  25. Li, S., Y. Tian, G. Lu, Y. Zhang, H. J. Xue, J.-Q. Wang, and X.-J. Jing, "A new kind of non-acoustic speech acquisition method based on millimeter waveradar," *Progress In Electromagnetics Research*, Vol. 130, 17–40, 2012.
  26. Crocco, L., F. Soldovieri, T. Millington, and N. J. Cassidy, "Bistatic tomographic GPR imaging for incipient pipeline leakage evaluation," *Progress In Electromagnetics Research*, Vol. 101, 307–321, 2010.
  27. Catapano, I., F. Soldovieri, and L. Crocco, "On the feasibility of the linear sampling method for 3D GPR surveys," *Progress In Electromagnetics Research*, Vol. 118, 185–203, 2011.

28. Van den Bosch, I., S. Lambot, M. Acheroy, I. Huynen, and P. Druyts, "Accurate and efficient modeling of monostatic GPR signal of dielectric targets buried in stratified media," *Journal of Electromagnetic Waves and Applications*, Vol. 20, No. 3, 283–290, 2006.
29. Zhu, Q. and L. M. Collins, "Application of feature extraction methods for landmine detection using the Wichmann/Niitek ground-penetrating radar," *IEEE Trans. Geosci. Remote Sensing*, Vol. 43, No. 1, 81–85, 2005.
30. Van der Merwe, A. and J. Gupta, "A novel signal processing technique for clutter reduction in GPR measurements of small, shallow land mines," *IEEE Trans. Geosci. Remote Sensing*, Vol. 38, No. 6, 2627–2637, 2000.
31. Nishimoto, M., S. Ueno, and Y. Kimura, "Feature extraction from GRP data for identification of landmine-like objects under rough ground surface," *Journal of Electromagnetic Waves and Applications*, Vol. 20, No. 12, 1577–1586, 2006.
32. Gader, P. D., M. Mystkowski, and Y. Zhao, "Landmine detection with ground penetrating radar using hidden Markov models," *IEEE Trans. Geosci. Remote Sens.*, Vol. 39, No. 6, 1231–1244, 2001.
33. Savelyev, T. G., L. van Kempen, H. Sahli, J. Sachs, and M. Sato, "Investigation of time-frequency features for GPR landmine discrimination," *IEEE Trans. Geosci. Remote Sensing*, Vol. 45, No. 1, 118–129, 2007.
34. Ho, K. C., L. M. Collins, L. G. Huettel, and P. D. Gader, "Discrimination mode processing for EMI and GPR sensors for hand-held landmine detection," *IEEE Trans. Geosci. Remote Sensing*, Vol. 42, No. 1, 249–263, 2004.
35. Lopera, O., E. C. Slob, N. Milisavljević, and S. Lambot, "Filtering soil surface and antenna effects from GPR data to enhance landmine detection," *IEEE Trans. Geosci. Remote Sensing*, Vol. 45, No. 3, 707–717, 2007.
36. Groenenboom, J. and A. Yarovoy, "Data processing and imaging in GPR system dedicated for landmine detection," *Sub. Sens. Tech. App.*, Vol. 3, No. 4, 2002.
37. Nishimoto, M. and V. Jandieri, "Ground clutter reduction from GPR data for identification of shallowly buried landmines," *IEICE Trans. Electron.*, Vol. E93-C, No. 1, 85–88, 2010.
38. Sun, Y. and J. Li, "Time-frequency analysis for plastic landmine detection via forward-looking ground penetrating radar," *IEE Proc. — Radar Sonar Navig.*, Vol. 150, No. 4, 253–261, 2003.

39. Tugac, S. and M. Efe, "Radar target detection using hidden Markov models," *Progress In Electromagnetics Research B*, Vol. 44, 241–259, 2012.
40. Wu, J. and M. Tian, "Landmine recognition research based on SVM," *Chinese J. Sci. Inst.*, Vol. 30, No. 7, 1487–1491, 2009.
41. Wilson, J. N., P. Gader, W.-H. Lee, H. Frigui, and K. C. Ho, "A large-scale systematic evaluation of algorithms using ground-penetrating radar for landmine detection and discrimination," *IEEE Trans. Geosci. Remote Sens.*, Vol. 45, No. 8, 2560–2572, 2007.
42. Jang, G., K. Kim, and K. H. Ko, "Multi-feature based landmine identification using ground penetrating radar," *3rd International Asia-Pacific Conference on Synthetic Aperture Radar (APSAR)*, 1–3, 2011.
43. Brunzell, H., "Detection of shallowly buried objects using impulse radar," *IEEE Trans. Geosci. Remote Sens.*, Vol. 37, No. 2, 875–886, 1999.
44. Iqbal, M., J. Chen, W. Yang, P. Wang, and B. Sun, "Kalman filter for removal of scalloping and inter-scan banding in scansar images," *Progress In Electromagnetics Research*, Vol. 132, 443–461, 2012.
45. Subrahmanyam, G. R. K. S., "A recursive filter for despeckling SAR Images," *IEEE Trans. Image Process.*, Vol. 17, 1969–1974, 2008.
46. Noh, S. Y., J. B. Park, and Y. H. Joo, "Intelligent tracking algorithm for maneuvering target using Kalman filter with fuzzy gain," *IET Radar, Sonar and Navigation*, Vol. 1, 241–247, 2007.
47. Pathirana, P. N. and A. V. Savkin, "Radar target tracking via robust linear filtering," *IEEE Signal Process. Lett.*, Vol. 14, 1028–1031, 2007.
48. Yardim, C., P. Gerstoft, and W. S. Hodgkiss, "Tracking Refractivity from clutter using Kalman and particle filters," *IEEE Trans. Antennas Propag.*, Vol. 56, 1058–1070, 2008.
49. Huang, C.-W. and K.-C. Lee, "Application of Ica technique to PCA based radar target recognition," *Progress In Electromagnetics Research*, Vol. 105, 157–170, 2010.
50. Riaz, M. M. and A. Ghafoor, "Principle component analysis and fuzzy logic based through wall image enhancement," *Progress In Electromagnetics Research*, Vol. 127, 461–478, 2012.
51. Zhang, Y., L. Wu, and S. Wang, "Magnetic resonance brain image classification by an improved artificial bee colony algorithm,"

- Progress In Electromagnetics Research*, Vol. 116, 65–79, 2011.
52. Zhang, Y. and L. Wu, “An Mr brain images classifier via principal component analysis and kernel support vector machine,” *Progress In Electromagnetics Research*, Vol. 130, 369–388, 2012.
  53. Chan, S.-C. and K.-C. Lee, “Radar target identification by kernel principal component analysis on RCS,” *Journal of Electromagnetic Waves and Applications*, Vol. 26, No. 1, 64–74, 2012.
  54. Wu, J., Z. Li, Y. Huang, Q. H. Liu, and J. Yang, “Processing one-stationary bistatic SAR data using inverse scaled Fourier transform,” *Progress In Electromagnetics Research*, Vol. 129, 143–159, 2012.
  55. Liu, Z., Q. H. Liu, C.-H. Zhu, and J. Yang, “A fast inverse polynomial reconstruction method based on conformal Fourier transformation,” *Progress In Electromagnetics Research*, Vol. 122, 119–136, 2012.
  56. Zavargo-Peche, L., A. Ortega-Monux, J. G. Wanguemert-Perez, and I. Molina-Fernandez, “Fourier based combined techniques to design novel sub-wavelength optical integrated devices,” *Progress In Electromagnetics Research*, Vol. 123, 447–465, 2012.
  57. Lee, J.-H., S.-W. Cho, S.-H. Park, and K.-T. Kim, “Performance analysis of radar target recognition using natural frequency: Frequency domain approach,” *Progress In Electromagnetics Research*, Vol. 132, 315–345, 2012.
  58. Ko, K. H., G. Jang, K. Park, and K. Kim, “GPR-based landmine detection and identification using multiple features,” *Int. J. Antennas Propag.*, Vol. 2012, 1–7, 2012.
  59. Zhu, X., Z. Zhao, W. Yang, Y. Zhang, Z.-P. Nie, and Q. H. Liu, “Iterative time-reversal mirror method for imaging the buried object beneath rough ground surface,” *Progress In Electromagnetics Research*, Vol. 117, 19–33, 2011.
  60. Li, J., B. Wei, Q. He, L.-X. Guo, and D.-B. Ge, “Time-domain iterative physical optics method for analysis of EM scattering from the target half buried in rough surface: PEC case,” *Progress In Electromagnetics Research*, Vol. 121, 391–408, 2011.